Temporal Upsampling Integration into a Microgrid Simulation Framework

H. Mankle, B. DuPont, and B. Robertson

Abstract—**As wave energy technology advances, there is a growing need for standardized methods to integrate into grid systems, including how to represent free surface time series for finite durations. Accurately representing the ocean wave variation is crucial for advanced controls and power systems modeling. However, the current method to model representative wave conditions calculate wave spectra using low temporal data and frequency-domain calculations which are not sufficient to capture the stochastic short-term variability. The issue with this practice is that spectrums are then used to predict the efficiency of systems that will not accurately capture the variability of waves in short timeframes. Creating a standardized methodology to increase the temporal resolution of metocean conditions to inform model development can provide better forecasting of power production. In this paper we present the implementation of an upsampling methodology into a larger microgrid simulation framework and show the significant increase in short-term variability for power generated by the Laboratory Upgrade Point Absorber.**

Index Terms—**Temporal resolution, wave energy converter, microgrids**

I. Introduction

THERE is a growing number of international communities investing in distributed energy resources (DERs) to power localized microgrids, providing increased energy security, diversity, and resilience [1]. With a large percentage of the population living near ocean coastlines, the growing threat of climate change and increased frequency of natural disasters highlights the potential importance of localized power generation.

This paper has been subjected to single-blind peer review. This paper is based upon work supported by the United States Department of Energy under Award Number DE-EE0009445. Neither the United States Government nor any agency thereof, nor any of their employees, makes any warranty, expressed or implied, or assumes any legal liability or responsibility for the accuracy, completeness, or usefulness of any information, apparatus, product, or process disclosed, or represents that its use would not infringe upon privately owned rights. Reference herein to any specific commercial product, process, or service by trade name, trademark, manufacturer, or otherwise does not necessarily constitute or imply its endorsement, recommendation, or favoring by the United States Government or any agency thereof. The views and opinions of the authors expressed herein do not necessarily state or reflect those of the United States Government or any agency thereof

H. Mankle and B. DuPont are with the Pacific Marine Energy Center and the School of Mechanical, Industrial, and Manufacturing Engineering, Oregon State University, Corvallis, OR 97331, United States (e-mails: mankleh@oregonstate.edu, bryony.dupont@oregonstate.edu).

B. Robertson is with the Pacific Marine Energy Center and the School of Civil and Construction Engineering, Oregon State University, Corvallis, OR, 97331, United States (e-mail: ryson.robertson@oregonstate.edu).

Digital Object Identifier:
https://doi.org/10.36688/ewtec-2023-564

Marine renewable energy can complement traditional renewable energy (i.e. wind and solar) in DERs by incorporating predictable and reliable energy in locations with marine hydrokinetic resources.

Distributed energy systems will need to be designed explicitly for the inclusion of marine renewable energy, as the power requirements for these systems are defined by local utilities. Therefore, advanced modeling approaches will become increasingly necessary. The objective of this paper is to present how a temporal upsampling methodology can be implemented into a larger framework to model microgrid projects to explore the sizing, design, and power stability of marine energy grids. Temporal resolutions of free-surface elevation time series must be statistically accurate to generate predictions with realistic variability for the power outputs of a wave energy converter (WEC).

Of the research conducted on DERs, only a small fraction consider wave energy. Prior literature of DERs with marine energy have discussed preliminary investigations of economic, technical, and design feasibility. These studies largely convey the high potential for localized grids and the synergies between solar, wind, and wave energy technologies [2]–[4]. Jahangir et al. perform techno-economic studies of hybrid energy systems and find the inclusion of wave energy to increase economic efficiency, specifically in areas where wind and solar resources are reduced [2]. Reikard et al. investigate a hybrid grid with wind, wave, and solar in the Northwest United States to find how geographic spreading and the addition of wave energy affect the power smoothing effects on the grid. Incorporating wave energy into the grid resulted in a reduction of localized noise and provided a smoother and more predictable power output than that of wind and solar technology [3]. Robertson et al. created DERs models with the inclusion of micro-hydro and wave energy in an effort to mitigate a remote community's use of diesel fuel [4]. Allowable-cost analysis conducted on the community did show reduced reliance on diesel fuel generation with the addition of wave energy and micro-hydro while continuing to provide further economic opportunities.

Although the addition of wave energy in DERs shows promise, the incorporation needs to adhere to grid requirements. That is, the power derived from wave energy converters has to align with the design of the distributed energy system. Said and Ringwood [5] provide a comprehensive review on the aspects of WEC grid integration and current research gaps. Power fluctuations is of concern and could cause damage to existing grids, emphasizing the need for

efficient control and energy storage to minimize these fluctuations. Another gap noted in the review is the exclusion of hydrodynamic characteristics and the use of complex WEC models. This can have significant effects on the performance of WECs depending on the model simplifications.

Wave stochasticity included in time-resolved methods create realistic time series realizations with accurate free-surface variance. The phase-resolved deterministic amplitude scheme (DAS) is the most common method used to generate free-surface time series [6]–[9]. When the DAS method is used wave variation is low and subsequently decreases variability in the resulting power of the WEC [6]–[9]. Although this provides a good indicator of the performance of the WEC, these model simplifications can obfuscate the true power characteristics of a WEC; understanding this uncertainty is crucial for WEC integration at the DER systems level. Further information on the DAS method and generated time series can be found in Section II.

When considering a microgrid system or a larger grid system, understanding of power variation is crucial. Fig. 1 shows the different stages of wave energy conversion and the significance the modeling holds on the end-use. The hierarchy of conversion is based on a microgrid control hierarchy described in Rojas and Rousan [10]. They distinguish the tertiary control functions in this control level as the load forecasting, model-based control and optimization for energy dispatch. The temporal requirements are more flexible and are typically several minutes. The tertiary energy conversion in this paper represents the wave energy resource input into simulations studying the performance of WECs. Wave resources are commonly input into simulation as free-surface time series generated with low resolution data, i.e publicly available data of representative wave parameters calculated from 30-min to 1-hr averaging intervals [9]. Averaging interval is defined as the temporal time steps used to calculate representative wave parameters.

Secondary control in [10] refers to general load control and data acquisition that is vital for switching between modes of operation. Here, the temporal resolution is typically in seconds. The secondary energy conversion stage (fig. 1) takes the motion of the waves and converts the oscillations into mechanical power, followed by the conversion to electrical power using power take offs (PTOs). This stage is modeled using time-domain methods to simulate the WEC and assess the power performance. Mechanical power is often used as a metric in studies on hydrodynamics or early-phase design work whereas electrical power is a commonly used metric in control studies. This is commonly where simplifications occur due to the computational expense of time-domain modeling.

Lastly, Primary control governs the generators and provides protection to the grid system. The primary energy conversion occurs as the electrical power is sent to energy storage or the grid. In Section III, we highlight the additional power system tools required to incorporate a WEC model into a microgrid.

Previous literature established a need for a statistically accurate time-resolved method that properly represents wave stochasticity in finite durations [6]–[9]. Improving the resolution of wave inputs into simulations will provide a more realistic wave representation to better inform PTO and grid control models during the secondary and primary stages. This paper focuses on the variation of wave energy in the tertiary stage and the effects on mechanical power in the secondary stage. To increase variation, the random amplitude scheme (RAS) is used in the upsampling process to create statistically representative time-series for finite durations, providing higher temporal resolutions for short durations ($<$ 30 minutes) [6]–[9].

This paper describes the implementation of upsampled wave resource inputs to better inform a detailed power systems analysis of a mircogrid. Section II provides a brief description of the background and theory for generating free-surface time series. Section III presents the generalized upsampling process and how the time series can be incorporated into a larger microgrid analysis. Section IV describes the includes information on the WEC parameters and resource conditions used for analysis. Finally, Section V and Section VI presents our results and conclusions.

II. Background and theory

Both DAS and RAS time series are generated using the power spectra calculated from elevation measurements or phase-averaged models. Phase-averaged models assume the wave statistical properties are stationary within the averaging interval, typically defined as 1-3 hours, to produce power spectra using a large number of waves [11]. Wave spectral shapes include Bretschneider [12], JONSWAP [13], and the Pierson-Moskowitz (PM) [14]. Equations (1) - (5) describe the relationship between the PM and JONSWAP spectra. The JONSWAP spectrum simplifies to the PM spectrum when the peak enhancement factor (γ) is 1, representing a fully developed sea. For γ values > 1, the JONSWAP spectrum represents developing seas. All are common methods of modeling irregular waves which use significant wave height (H_s) and peak period (T_p) as inputs to calculate spectral densities [15].

For the purposes of this study, only the JONSWAP spectrum is used with γ, normalized frequency $\hat{f} = \frac{f}{f_p}$, and $f_p = \frac{1}{T_p}$:

$$S_{PM}(\hat{f}) = \frac{H_s^2}{3.2 f_p} \hat{f}^{-5} exp(-1.25\hat{f}^{-4}) \tag{1}$$

$$S_J(\hat{f}) = C_J . S_{PM}(\hat{f}) . \gamma^{-\frac{(\hat{f}-1)^2}{2\sigma^2}} \tag{2}$$

$$C_J = \frac{H_s^2}{16 m_0} \tag{3}$$

$$m_0 = \int_0^\infty S_{PM}(\hat{f}) . \gamma^{-\frac{(\hat{f}-1)^2}{2\sigma^2}} \, d\hat{f} \tag{4}$$

$$\sigma = \begin{cases} \sigma_a \text{ for } \hat{f} \leq 1 (\text{typically: } 0.07) \\ \sigma_b \text{ for } \hat{f} > 1 (\text{typically: } 0.09) \end{cases} \tag{5}$$

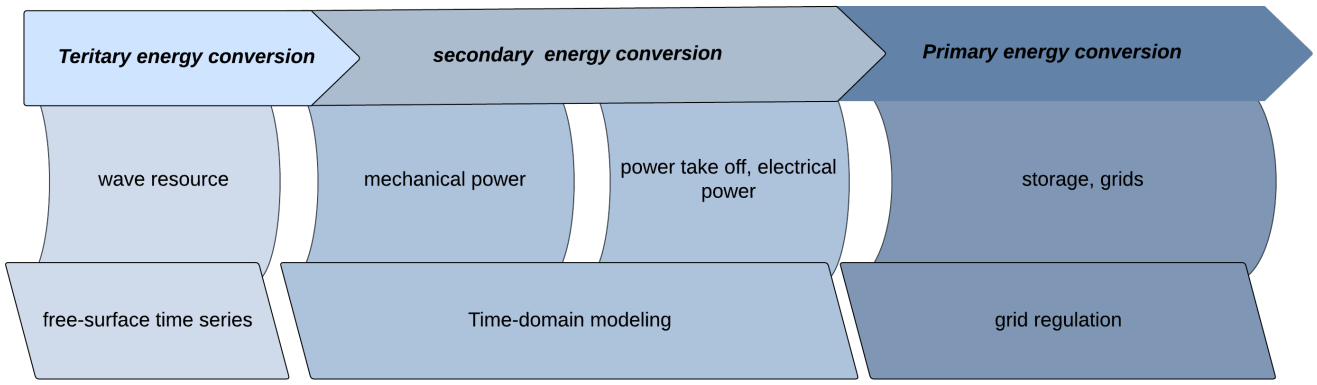

Fig. 1. Energy conversion DRAFT

where the scaling coefficient, C_J, is calculated by integration which accounts for the peak enhancement factor. Further detail on the spectra can be found at [16].

Time series generated using the DAS method randomly assign phases (ϕ_k) over a uniform-distribution from $[0; 2\pi]$ and harmonic sinusoidal wave components are summed with random phases and spectra-derived amplitudes. Equation (6) defines the deterministic time series η_{t_i} for a given spectral density function $S(f)$ of a finite length $T = N\Delta t$.

$$\eta_{t_i} = \sum_{k=1}^{M/2} A_k \cos\left(2\pi f_k t_i + \phi_k\right) \tag{6}$$

with the ith and kth elements $i = 1 \ldots N$ and $k = 1, \ldots, M/2$, where $M/2$ is the number of discrete frequency components (typically M=N). The timestep $t_i = i\Delta t$, frequency $f_k = k\Delta f$ where, $\Delta f = \frac{1}{M\Delta t}$, and amplitude $A_k = \sqrt{2S(f_k)\Delta f}$.

DAS provides accurate estimates for longer-term metrics but does not represent the true variation of waves [6]–[9]. The spectral shape and variance will remain constant with the DAS method unless the time series duration reaches infinity [6]. Realistic time series instances should differ and vary from the mean. Using DAS results in similar spectral moments and significant wave heights, even as the duration decreases.

As the name suggests, the random amplitude scheme (RAS) creates time series by randomly assigning amplitude components with variance provided by the spectral density function and following a gaussian distribution [6]–[9]. Equation (7) describes the RAS generated free-surface time series.

$$\eta_{t_i} = \sum_{k=1}^{M/2} a_k \cos\left(2\pi f_k t_i\right) + b_k \cos\left(2\pi f_k t_i\right) \tag{7}$$

$$A_k = \sqrt{a_k^2 + b_k^2} \tag{8}$$

where the amplitudes a_k, b_k are chosen randomly and follow a normal distribution with a standard deviation of $\sqrt{S(f_k)\Delta f}$ and a mean of zero.

Equation (6) and (7) are equivalent due to the relationship between a_k, b_k and A_k found in (8). When generating a RAS time series with (6) the phase is chosen randomly, following a uniform distribution from $[0; 2\pi]$, randomly selected A_k, and a Rayleigh distribution with a variance of $2S(f_k)\Delta f$.

Accurate wave statistics are maintained when generating time series with RAS, providing a more realistic stochastic gaussian process. If comparing H_s values calculated from multiple time series realizations, RAS generated H_s values will vary from the mean for each realization to better represent realistic time series for finite durations. Whereas DAS will produce H_s close to the mean of the realizations. Further information of the advantages and disadvantages of RAS and DAS can be found in [6].

III. Upsampling Implementation

Fig. 2 shows the implementation of a wave upsampling process into a wave-to-wire microgrid modeler and power system operator. This section provides a high level description of the incorporation of the upsampling methodology into a microgrid simulation framework is discussed.

A. Free-surface elevation time series generation

A 10-million time series ensemble was generated through Monte-Carlo simulation with (7) and linear wave theory to create an empirical probability distribution. Time series must be a realistic representation of the stochastic nature of waves to capture the influence of the wave field for WEC power generation. To prevent biases in the variance calculation in the time series generation, spectra calculated using (2) are kept at a constant high-resolution ($M = 2^{16}$) and sampling intervals. A random seed is retained for each time series and probability distributions for wave parameters are calculated (e.g. H_s and H_max). An example of a distribution from a seed can be found in Fig. 2 with vertical lines showing varying percentiles along the distribution.

The resulting distributions are a function of γ and the number of waves. The number of waves alters the calculations of representative wave parameters by defining the temporal time steps, moving forward we will call this the *averaging interval*. Further details on

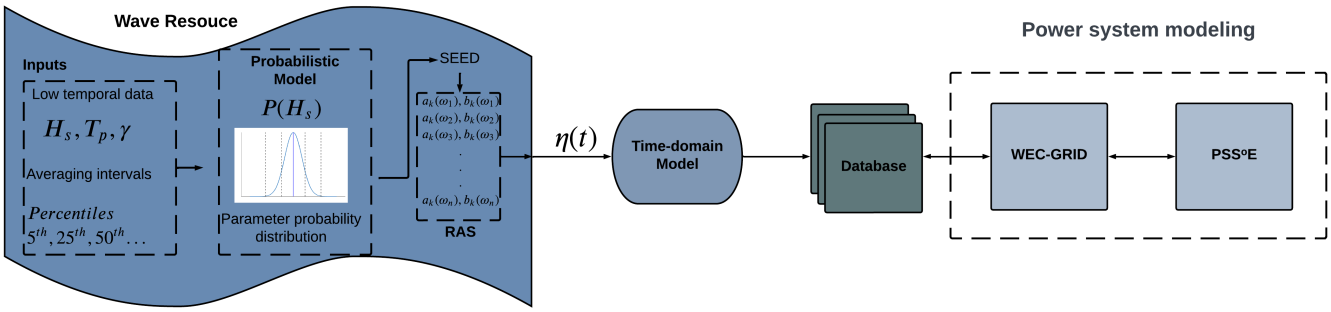

Fig. 2. Flowchart depicting the time series temporal upsampling methodology implementation in a larger microgrid simulation framework.

the probability model can be found in Mankle et al. [9] and the general process is shown in Fig. 2. Information from the probabilistic model is pulled corresponding to a seed and desired percentile. Due to the large size of the probabilistic model, which includes all realizations and percentiles, only select percentiles are pulled for a requested seed to save computational time.

H_s and T_p are user-defined and used to scale the free-surface time series from the probabilistic model. These wave parameters are location dependent, but typical T_p values are 6-20 s. The final averaging interval is determined by T_p and is scaled linearly; a 50-wave time series with a T_p of 8 s will have an averaging interval of 400 s while a 20-wave time series with a T_p of 8 s will have an averaging interval of 160 s. In following sections T_p values of 15 s and 11 s are used for verification and WEC simulation. The shortest averaging intervals in these analyses will be 5 minute and 3 minute respectfully.

Inputting the generated time series follows the general time-domain process of inputting free-surface time series. All user-defined parameters in this process are the distribution percentile, averaging interval, and spectrum peak enhancement factors. The five percentiles used are the $5th$, $25th$, $50th$, $75th$, and $95th$ percentiles.

B. Time-domain modeling

Frequency-domain modeling using linear forcing is a good early design methodology, but a WEC system must capture the nonlinearities to incorporate complex PTO configurations, viscous drag, and other nonlinear interactions. Equation (9) describes the force balance equation in the time-domain:

$$\begin{aligned}(M + A_\infty)\ddot{X}(t) =& F_{ex}(t) + F_{rad}(t) + F_{PTO}(t) \\ &+ F_{drag}(t) + F_{hs}(t) + F_m(t)\end{aligned} \tag{9}$$

$$F_{PTO}(t) = -B_{PTO}\dot{X}(t) - K_{PTO}X(t) \tag{10}$$

$$F_m(t) = -K_m X(t) \tag{11}$$

where M is the mass matrix, A_∞ is the added mass, and $\ddot{X}$ is the acceleration of the body. The terms on the right side are the external and reactionary forces acting on the body. The external loads include the hydrostatic force, F_{hs}, which is the variation of the hydrostatic pressure distribution; excitation force, F_{ex}, is the interaction between the incident waves against a static geometry; radiation force, F_{rad}, is the change in momentum of the fluid from the motion of the geometry; and the damping force, F_{drag}, is the viscous losses in the system. The linear reactionary power-take-off (PTO) force, F_{PTO} (10), is the sum of the reactionary forces from the controllable PTO system where B_{PTO} and K_{PTO} are the damping and spring coefficients respectively. Station keeping is emulated through the spring stiffness K_m and is a mooring constraint acting on the WEC to hold it in position.

Added mass, wave excitation force, and radiation are taken straight from the frequency-domain model [17], [18]. Further information on time-domain modeling can be found in [15] and [19].

C. Power systems modeling

WEC-Grid software presents an open-source framework for electro-mechanical power conversion by connecting the functionality of WEC-Sim with power flow software, which is not currently available elsewhere [20]. Power flow software is used by power system engineers to ensure grid stability through monitoring the energy demand and adjusting the loads.

Power flow tools are designed to simulate grids models that include information on the generators, electrical lines and loads to find stable solutions that don't compromise grid functionality. These tools can model tens to thousands of power system buses and generators. The power system tool currently implemented in the WEC-Grid framework is Siemens PSS®E (Fig. 2), a commercial software widely used in the power systems industry [21].

Other tools that could be incorporated into the WEC-Grid framework include the Micro Grid Renewable Integration Dispatch and Sizing (MiGRIDS) [22], and Python for Power System Analysis (PyPSA) [23]. MiGRIDs is a software designed to model islanded microgrid power systems and was developed by the Alaskan Center for Energy and Power (ACEP) [22]. When possible, local load and generation data can be leveraged to create realistic microgrid models. PyPSA is an open-source software that models smooth energy transitions for complex electricity networks [23]. Additional capabilities include renewable energy modeling and cost-optimizing for energy systems.

Modeling WECs in WEC-Sim largely focuses on the hydrodynamic interactions and requires further development to interface with effective power system

modeling tools. While PTO-Sim can calculate electrical power generated from a WEC, the electrical load is modeled as a fixed resistance and is unrealistic for control schemes connected to a grid with linear and nonlinear loads [24].

The wave-to-grid tool, WEC-Grid, acts as a software wrapper and communicates with the different software being used. WEC-Grid is run through an Anaconda environment using Jupyter notebooks as a user interface. Currently WEC-Sim is the largest computational cost and eliminating the need for the MATLAB GUI and running through the Anaconda environment significantly reduces the computational time.

To simulate power flows of WEC-powered microgrids, electrical power outputs from WEC-Sim are sent to a SQL database which communicates with the microgrid models (Fig. 2). The database shares data between WEC-Sim/PTO-Sim and WEC-Grid and provides time-domain-specific operation necessary for the microgrid simulation. The resolution of the WEC-Sim and PTO models often have timesteps 0.1 second. The outputs are then down-sampled to 5 minute intervals and accessed by WEC-Grid. Further information on the WEC-Grid framework can be found in Barajas-Ritchie et al. [20].

IV. Case Study

In this paper, the upsampling methodology is used to demonstrate the importance of temporal resolution for short-term modeling as part of a larger framework to simulate a microgrid system. Different temporal resolutions are used to generate free-surface time series with data from the PacWave South (PWS) open ocean wave energy test facility located off the coast of Newport, Oregon, USA (Fig. 3). PacWave is a grid-connected, 20 MW, 4-berth test facility in development with a partnership between the US Department of Energy, the State of Oregon, Oregon State University (OSU) and local stakeholders. The large renewable resources found in the Pacific Northwest of the US provides ample opportunities for marine renewable energy and offshore wind energy development [25].

To validate that the upsampling process produces higher variation for short durations, high resolution measurements collected near PWS with Surface Wave Instrument Floats with Tracking (SWIFT) buoys were used [26]. Data is collected in 10-minutes bursts and are sampled at 25 Hz. In this paper, the raw elevation time series recorded by the SWIFT buoys are used for analysis. To reduce complexity, wave statistics were calculated from the data are based on the assumption that the SWIFT buoy is stationary instead of free-floating [26]. Further information on data collection and specifications can be found in Thomson et al. [27].

A. Wave energy converter technology

The WEC used in this study is Oregon State University's (OSU) open-source Laboratory Upgrade Point Absorber (LUPA) (Fig. 4) [28]. LUPA is a 1 m laboratory-size WEC designed with three different operating modes that increase in complexity.

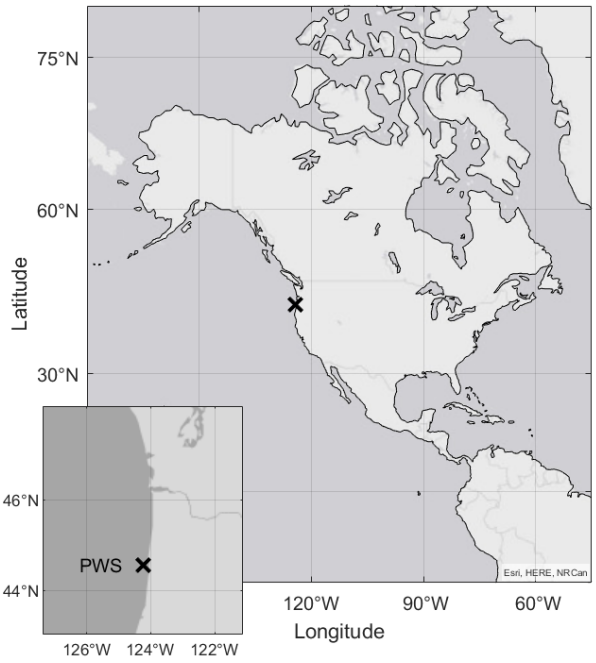

Fig. 3. Map of the the Americas with the location of the PacWave South test site [25].

TABLE I
Model properties of LUPA for time-domain simulations

Properties	Value	Unit
Float diameter	20	m
Float mass	$1.86 \cdot 10^6$	kg
Float height	14.2	m
Spar diameter	18.3	m
Spar mass	$1.42 \cdot 10^6$	kg
Spar height	73.2	m
PTO damping	300	N/m
PTO damping	10^4	$N \cdot s/m$

The three-modes include: single-body heave-only, two-body heave-only, and two-body 6 degrees of freedom. Both two-body configurations generate power through the relative displacement between the float and spar. Due to LUPA's modular design, research opportunities with LUPA include testing hull geometries, system operation degrees of freedom, PTO control system configuration, and mooring impacts. This study uses a 20 m field-size LUPA linearly scaled from the lab-size model I. Experimental validation of LUPA is on-going and further details on the experimental testing of the three modes can be found in Beringer et al. [29].

V. Results

In Fig. 5, real, high-resolution field measurements are compared against the upsampled parametric distributions of significant wave height to establish the need for higher resolution time series inputs into WEC-Sim. The blue x's are the significant wave heights calculated with different averaging intervals for a series of data recording spanning 6 hours. Each horizontal spread represents a single averaging interval. The average

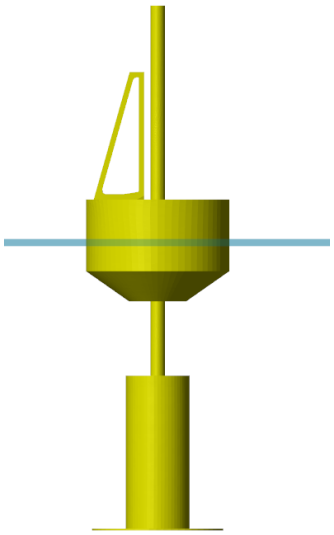

Fig. 4. WEC-Sim model of Oregon State University's Laboratory Upgrade Point Absorber [28].

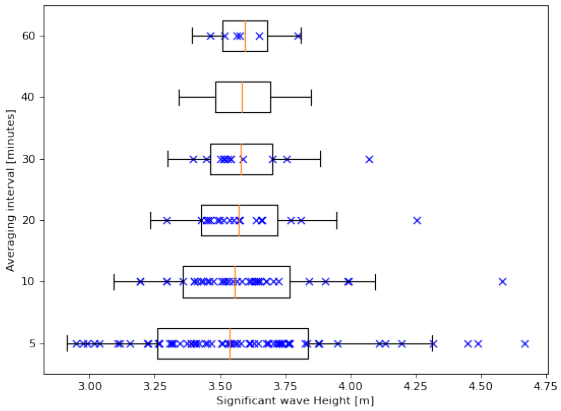

Fig. 5. Significant wave height distribution based on averaging interval. The whiskers on the plots represent the 5th and 95th percentiles. The boxes show the 25th and 75th percentiles while the red line is the 50th percentile. Blue x's are significant wave heights calculated based on averaging interval from high resolution data.

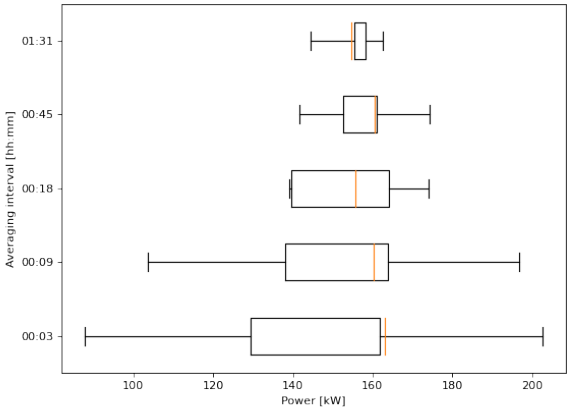

Fig. 6. Average power distribution based on averaging interval. The whiskers on the plots represent the 5th and 95th percentiles. The boxes show the 25th and 75th percentiles while the red line is the 50th percentile.

wave height for the hour-long upsampled averaging interval acted as the scaling term for the probabilistic distribution. The boxplots for each averaging interval shows the distribution of the 5th, 25th, 50th, 75th, and 95th percentiles. The 50th percentile is shown as a red line on the plots.

Most points of the SWIFT H_s values fit well within the 5th and 95th percentile from the probabilistic model in Fig. 5. The percentage of outliers increases from the 5 to 30 minute averaging intervals. The number of outliers only accounts for 4.2% of all of the H_s values with a 5 minute averaging interval. Although the 30 minute averaging interval only has one outlier, this still accounts for 8.3% of the H_s values.

Fig. 5 shows the increased variation of short averaging intervals that matches well with real, high-resolution data. As averaging intervals increase, variation decreases and starts to converge towards the mean H_s value.

To investigate the influence of averaging interval on power generation, the RAS-generated time-series were scaled with the most frequent sea state at PacWave South, where $H_s = 3$ m and $T_p = 11$ s and $\gamma = 3.3$ [30]. Seed 221112 from the probabilistic model was used to pull the time-series for the specified percentiles and used as the input for the WEC-Sim simulations. Simulation lengths calculated using a T_p of 11 seconds ranged from 3 minutes to 1 hour and 31 minutes.

Fig. 6 displays the average mechanical power generated from LUPA for different averaging intervals. The distribution follows the same trend as the significant wave height distribution from the probabilistic model. The variation between the 5th and 95th percentiles for the 3 minute averaging interval with a spread of 87.2 kW for average power, 130% greater than the spread of the 90 minute averaging interval. The 95th confidence interval decreases significantly with the 18 minute averaging interval, followed by a gradual decreases as the averaging interval increases.

VI. Conclusion

Research for marine energy technology has shifted in recent years from developing strictly utility-size technology to investing in technology that can power a range of applications with smaller power demand. The increasing global support for more localized microgrids provides marine renewable energy technology an opportunity to complement existing distributed energy resources. Exisiting DERs are often comprised of wind and solar technology, but locations with a marine energy resource have the opportunity to diversify their energy portfolio. However, there is a need for standardized methodology in order for accurate resource and power forecasting.

In this paper, we highlight the need for higher-resolution time series input into a larger WEC modeling framework. Variability in significant wave height

compared against real high resolution data showed significant increase in variation for the smallest averaging intervals. Applying the probabilistic distributions to generate free surface time series also showed significant increase in variability for shorter averaging intervals.

Looking at the impact low variation can have on the larger microgrid framework, the significant decrease in variation for the larger can lead to misrepresentation of power systems modeling. Implementing statistically accurate, temporally upsampled time series into time-domain models (i.e. WEC-Sim [16]) will provide short-term predictions of the wave conditions, hydrodynamic forcing, and WEC performance necessary for the design, operation, and survivability of marine renewable energy technologies.

ACKNOWLEDGEMENT

This work was supported in part by the US Department of Energy, Office of Energy Efficiency and Renewable Energy, Water Power Technology Office under the grant number DEEE0009445.

REFERENCES

[1] M. Warneryd, M. Håkansson, and K. Karltorp, "Unpacking the complexity of community microgrids: A review of institutions' roles for development of microgrids," *Renewable and Sustainable Energy Reviews*, vol. 121, p. 109690, 2020. [Online]. Available: https://www.sciencedirect.com/science/article/pii/S1364032119308950

[2] M. H. Jahangir, S. Fakouriyan, M. A. Vaziri Rad, and H. Dehghan, "Feasibility study of on/off grid large-scale PV/WT/WEC hybrid energy system in coastal cities: A case-based research," *Renewable Energy*, vol. 162, pp. 2075–2095, 2020. [Online]. Available: https://www.sciencedirect.com/science/article/pii/S0960148120315573

[3] G. Reikard, B. Robertson, and J.-R. Bidlot, "Combining wave energy with wind and solar: Short-term forecasting," *Renewable Energy*, vol. 81, pp. 442–456, Sep. 2015. [Online]. Available: https://www.sciencedirect.com/science/article/pii/S0960148115002141

[4] B. Robertson, J. Bekker, and B. Buckham, "Renewable integration for remote communities: Comparative allowable cost analyses for hydro, solar and wave energy," *Applied Energy*, vol. 264, p. 114677, Apr. 2020. [Online]. Available: https://www.sciencedirect.com/science/article/pii/S0306261920301896

[5] H. A. Said and J. V. Ringwood, "Grid integration aspects of wave energy—Overview and perspectives," *IET Renewable Power Generation*, vol. 15, no. 14, pp. 3045–3064, 2021, _eprint: https://onlinelibrary.wiley.com/doi/pdf/10.1049/rpg2.12179. [Online]. Available: https://onlinelibrary.wiley.com/doi/abs/10.1049/rpg2.12179

[6] A. Mérigaud and J. V. Ringwood, "Free-Surface Time-Series Generation for Wave Energy Applications," *IEEE Journal of Oceanic Engineering*, vol. 43, no. 1, pp. 19–35, Jan. 2018, conference Name: IEEE Journal of Oceanic Engineering.

[7] M. Tucker, P. Challenor, and D. Carter, "Numerical simulation of a random sea: a common error and its effect upon wave group statistics," *Applied Ocean Research*, vol. 6, no. 2, pp. 118–122, 1984.

[8] J. Saulnier, B., P. Ricci, A. Clément, and A. d. O. Falcaõ, "Mean Power Output Estimation of WECs in Simulated Sea," in *Proceedings of The 8th European Wave and Tidal Energy Conference (EWTEC 2009*, vol. Vol. 710, Uppsala, Sweden, 2009.

[9] H. Mankle, P. Branson, B. DuPont, and B. Robertson, "Temporal Upsampling of Wave Parameters and Impact on Time-Domain Floating Body Response and Wave Power," *Journal of Ocean Engineering and Marine Energy[Manuscript accepted for publication]*, 2023.

[10] A. Rojas and T. Rousan, "Microgrid Control Strategy: Derived from Stakeholder Requirements Analysis," *IEEE Power and Energy Magazine*, vol. 15, no. 4, pp. 72–79, Jul. 2017, conference Name: IEEE Power and Energy Magazine.

[11] B. Robertson, "Wave Energy Assessments: Quantifying the Resource and Understanding the Uncertainty," in *Marine Renewable Energy: Resource Characterization and Physical Effects*, Z. Yang and A. Copping, Eds. Cham: Springer International Publishing, 2017, pp. 1–36. [Online]. Available: https://doi.org/10.1007/978-3-319-53536-4_1

[12] C. L. Bretschneider, *Wave Variability and Wave Spectra for Wind-generated Gravity Waves*. The Board, 1959, google-Books-ID: ReuL8Opx07kC.

[13] K. Hasselmann, T. P. Barnett, E. Bouws, H. Carlson, D. E. Cartwright, K. Enke, J. A. Ewing, A. Gienapp, D. E. Hasselmann, and P. Kruseman, "Measurements of wind-wave growth and swell decay during the Joint North Sea Wave Project (JONSWAP)." *Ergaenzungsheft zur Deutschen Hydrographischen Zeitschrift, Reihe A*, 1973.

[14] W. J. Pierson Jr. and L. Moskowitz, "A proposed spectral form for fully developed wind seas based on the similarity theory of S. A. Kitaigorodskii," *Journal of Geophysical Research (1896-1977)*, vol. 69, no. 24, pp. 5181–5190, 1964. [Online]. Available: https://onlinelibrary.wiley.com/doi/abs/10.1029/JZ069i024p05181

[15] P. Ricci, "Time-Domain Models," in *Numerical Modelling of Wave Energy Converters*. Elsevier, 2016, pp. 31–66. [Online]. Available: https://linkinghub.elsevier.com/retrieve/pii/B9780128032107000037

[16] K. Ruehl, A. Keester, C. A. M. Ströfer, nathanmtom, M. Topper, M. Lawson, dforbush2, B. A. Ling, jtgrasb, j vanrij, Sal, jhbates, D. Ogden, L. Nguyen, Jeffalo1, J. Leon, sedwardsand, E. F. Alves, crobarcro, emiliofa, ratanakso, A. Rashid, Aquaharmonics, F. Sauer, M. Ancellin, NREL-Jim-McNally, SiHeTh, gparisella, M. Hall, and yuyihsiang, "WEC-Sim/WEC-Sim: WEC-Sim v5.0.1," Sep. 2022. [Online]. Available: https://zenodo.org/record/7121186

[17] M. Alves, "Frequency-Domain Models," in *Numerical Modelling of Wave Energy Converters*. Academic Press, 2016, pp. 11–30.

[18] B. Bosma, Z. Zhang, T. K. Brekken, H. T. Ozkan-Haller, C. McNatt, and S. C. Yim, "Wave energy converter modeling in the frequency domain: A design guide," in *2012 IEEE Energy Conversion Congress and Exposition (ECCE)*. Raleigh, NC, USA: IEEE, Sep. 2012, pp. 2099–2106. [Online]. Available: http://ieeexplore.ieee.org/document/6342553/

[19] A. Babarit, J. Hals, M. J. Muliawan, A. Kurniawan, T. Moan, and J. Krokstad, "Numerical benchmarking study of a selection of wave energy converters," *Renewable Energy*, vol. 41, pp. 44–63, May 2012. [Online]. Available: https://www.sciencedirect.com/science/article/pii/S0960148111005672

[20] A. Barajas-Ritchie, D. Jackson, E. Cotilla-Sanchez, and Y. Cao, "Open-Source Steady-State Models for Integration of Wave Energy Converter into Microgrids," in *IEEE Sponsored Conference International Conference on Future Energy Solutions [under review]*, 2023.

[21] "PSS®E – transmission planning and analysis - PSS® power system simulation and modeling software - Global." [Online]. Available: https://www.siemens.com/global/en/products/energy/grid-software/planning/pss-software/pss-e.html

[22] J. Vandermeer and M. Mueller-Stoffles, "MiGRIDS," 2022, original-date: 2017-09-06T16:07:10Z. [Online]. Available: https://github.com/acep-uaf/MiGRIDS

[23] T. Brown, J. Hörsch, and D. Schlachtberger, "PyPSA: Python for Power System Analysis," *Journal of Open Research Software*, vol. 6, no. 1, p. 4, Jan. 2018. [Online]. Available: https://openresearchsoftware.metajnl.com/article/10.5334/jors.188/

[24] R. So, A. Simmons, T. Brekken, K. Ruehl, and C. Michelen, "Development of pto-sim: A power performance module for the open-source wave energy converter code wec-sim," in *International Conference on Offshore Mechanics and Arctic Engineering*, vol. 56574. American Society of Mechanical Engineers, 2015, p. V009T09A032.

[25] "PacWave – TESTING WAVE ENERGY FOR THE FUTURE." [Online]. Available: https://pacwaveenergy.org/

[26] J. Thomson, A. Brown, T. Ozkan-Haller, A. Ellenson, and M. Haller, "Extreme Conditions at Wave Energy Sites," *Marine Energy Technology Symposium (METS)*, p. 4, 2016.

[27] J. Thomson, "Wave Breaking Dissipation Observed with "SWIFT" Drifters," *Journal of Atmospheric and Oceanic Technology*, vol. 29, no. 12, pp. 1866–1882, Dec. 2012. [Online]. Available: http://journals.ametsoc.org/doi/10.1175/JTECH-D-12-00018.1

[28] B. Bosma, C. Beringer, M. Leary, and B. Robertson, "Design and modeling of a laboratory scale WEC point absorber," in *Proc. of the 14th European Wave and Tidal Energy Conference*, 2021, p. 9.

[29] C. Beringer, B. Bosma, and B. Robertson, "Degrees of freedom effects on a laboratory scale WEC point absorber," in *Proc. of the 15th European Wave and Tidal Energy Conference*, 2023.

[30] B. Robertson, G. Dunkle, J. Gadasi, G. Garcia-Medina, and Z. Yang, "Holistic marine energy resource assessments: A wave and offshore wind perspective of metocean conditions," *Renewable Energy*, vol. 170, pp. 286–301, Jun. 2021. [Online]. Available: https://www.sciencedirect.com/science/article/pii/S096014812100149X